Heliyon 10 (2024) e24557

Contents lists available at ScienceDirect

Heliyon

journal homepage: www.cell.com/heliyon

Research article

Longitudinal analysis of T2 relaxation time variations following radiotherapy for prostate cancer

Pavla Hanzlikova [a,b,1], Dominik Vilimek [c,*,1], Radana Vilimkova Kahankova [c], Martina Ladrova [c], Valeria Skopelidou [d,e], Zuzana Ruzickova [f,g], Radek Martinek [c], Jakub Cvek [f,g]

[a] Department of Radiology, University Hospital Ostrava, Czech Republic
[b] Department of Imaging Methods, Faculty of Medicine, University of Ostrava, Ostrava, Czech Republic
[c] Department of Cybernetics and Biomedical Engineering, Faculty of Electrical Engineering and Computer Science, VSB - Technical University of Ostrava, 17. listopadu 15, Ostrava – Poruba, 708 00, Czech Republic
[d] Institute of Molecular and Clinical Pathology and Medical Genetics, University Hospital Ostrava, 70852, Ostrava, Czech Republic
[e] Institute of Molecular and Clinical Pathology and Medical Genetics, Faculty of Medicine, University of Ostrava, 70300, Ostrava, Czech Republic
[f] Faculty of Medicine, University of Ostrava, 70300 Ostrava, Czech Republic
[g] Department of Oncology, University Hospital Ostrava, 70852 Ostrava, Czech Republic

ARTICLE INFO

Keywords:
Prostate cancer
Radiation therapy
Quantitative MRI
T2 relaxation times
Treatment response

ABSTRACT

Aim of this paper is to evaluate short and long-term changes in T_2 relaxation times after radiotherapy in patients with low and intermediate risk localized prostate cancer. A total of 24 patients were selected for this retrospective study. Each participant underwent 1.5T magnetic resonance imaging on seven separate occasions: initially after the implantation of gold fiducials, the required step for Cyberknife therapy guidance, followed by MRI scans two weeks post-therapy and monthly thereafter. As part of each MRI scan, the prostate region was manually delineated, and the T_2 relaxation times were calculated for quantitative analysis. The T_2 relaxation times between individual follow-ups were analyzed using Repeated Measures Analysis of Variance that revealed a significant difference across all measurements ($F(6, 120) = 0.611$, $p << 0.001$). A Bonferroni post hoc test revealed significant differences in median T_2 values between the baseline and subsequent measurements, particularly between pre-therapy (M_0) and two weeks post-therapy (M_1), as well as during the monthly interval checks (M_2 - M_6). Some cases showed a delayed decrease in relaxation times, indicating the prolonged effects of therapy. The changes in T_2 values during the course of radiotherapy can help in monitoring radiotherapy response in unconfirmed patients, quantifying the scarring process, and recognizing the therapy failure.

* Corresponding author.
E-mail addresses: pavla.hanzlikova@fno.cz (P. Hanzlikova), dominik.vilimek@vsb.cz (D. Vilimek), radana.vilimkova.kahankova@vsb.cz (R. Vilimkova Kahankova), martina.ladrova@vsb.cz (M. Ladrova), valeria.skopelidou@fno.cz (V. Skopelidou), zuzana.ruzickova@fno.cz (Z. Ruzickova), radek.martinek@vsb.cz (R. Martinek), jakub.cvek@fno.cz (J. Cvek).
[1] These authors contributed equally to this paper.

https://doi.org/10.1016/j.heliyon.2024.e24557
Received 7 July 2023; Received in revised form 2 December 2023; Accepted 10 January 2024

Available online 15 January 2024

1. Introduction

Prostate cancer (PCa) is one of the most common malignant tumors in middle-aged and elderly men [1]. There is a clearly increasing incidence of this disease, which threatens not only the physical but also the mental health of these patients [2]. Commonly used screening methods based on prostate-specific antigen (PSA) do not provide sufficient information about the presence of PCa and there are many factors influencing the results [3]. Moreover, deciding on the necessity of a biopsy is difficult, as finding a compromise between obtaining accurate results and minimizing harm to the patient, along with potential health complications, proves challenging [3].

Magnetic Resonance Imaging (MRI) plays a crucial role in detecting PCa, as it allows for the quantitative assessment of tissue status. This non-invasive technique provides high soft-tissue contrast and resolution, and is free of radiation compared to widely used computed tomography (CT) [3]. Examinations using MRI combined with PSA blood test or transrectal ultrasound biopsy (TRUS) reported a superior PCa detection rate [4–6] and recent 10-year follow-up study showed that multiparametric MRI is a key tool to establish risk groups of PCa patients and thus, optimize their radiotherapy [7].

However, diagnosis using MRI is time-consuming and requires substantial expertise due to the large number of images that need to be read. Moreover, image analysis is susceptible to interpretation errors due to observer limitations and clinical complexity [4,8]. In clinical practice, prostate MRI is reported using the Prostate Imaging and Data Reporting System (PI_RADS) v2.1 [9], which relies upon mainly subjective analysis of MR imaging findings, with very few incorporated quantitative features, such as size and volume of tumor, mean value of Apparent Diffusion Coefficient (ADC), or length of capsular contact [10].

Relaxometry is another effective way to objectively describe changes in the tissue behavior. It allows to reflect tissue properties and histological changes by the measurement of tissue relaxation times, such as T_1, T_2, and T_2^*, with the possibility to differentiate grades of PCa, especially in combination with ADC mapping. Previous studies showed that the quantitative T_2 mapping allows distinguishing between prostate cancer and normal gland tissue, or benign prostatic hyperplasia nodes [11], even that T_2 and T_2^* are shortened in more aggressive cancers compared to low-grade cancers [12]. The method also proved to be highly reproducible [10] and showed promising predictive ability in MR-guided PCa radiotherapy [13].

T_2 relaxometry is an MRI technique that analyzes the transverse relaxation time in order to determine the properties of the tissue [14,15]. This method enhances the interpretation of MRI data by distinguishing separate contributing factors, such as spin relaxation times. By generating T_2 maps, it enables more precise tissue characterization, enhances contrast between different tissue types, and establishes a clearer relationship between the MRI signal variations and the underlying microanatomical structures. Furthermore, the quantitative nature of the data enables easy comparisons across longitudinal time points [16].

In general, T_2 mapping could provide insights into the changes that occur in the tissue composition. For example, when tumor destruction and associated reparative processes lead to changes in the composition of the tissues. Therefore, the primary objective of this research is to rigorously examine and quantify the short and long-term changes in T_2 relaxation times following radiotherapy using CyberKnife in patients with biopsy-confirmed low- and intermediate-risk prostate cancer.

In 2013, this method for image-guided robotic Stereotactic Body Radiation Therapy (SBRT) was listed by American Society for Radiation Oncology as an alternative for low- and intermediate-risk PCa. The SBRT is a technique using only radiation beam (instead of body cuts) and focus of radiations with high power of energy on small area of the body, which allows to minimize damage of close healthy tissue [17]. Moreover, CyberKnife has an advantage of real-time tracking of the dynamic tumor position for realigning the beam, short treatment time, high dose gradient, treatment accuracy, and cost–effectiveness compared with other radiotherapy equipment [18].

It was found that prostate SBRT affords appropriate biochemical control with few high-grade toxicities [19]. However, the presence of late toxicity should be observed minimally for 2 years after the treatment, which is still short follow-up period to evaluate efficacy; relapse of PCa can be obvious even after 5 years of latency [20]. A recent 36-month follow-up study [21] confirmed an excellent control of CyberKnife treatment with 35–36.25 Gy in five fractions with low toxicity in low- to intermediate-risk PCa patients. No dose-related differences in biochemical control and overall survival were found. Also, the 5-year follow-up study [22] presented excellent long-term outcomes in all-risk groups of patients after CyberKnife treatment with the disease-specific survival rate of the whole cohort of 99.1%, as only two from 110 high-risk patients died due to PCa.

By utilizing T_2 mapping via 1.5T MRI, this study aims to offer a detailed, longitudinal analysis of the changes within the prostate gland, providing valuable insights into the water content or changes in the extracellular matrix. The main contributions of this study are as follows:

- *Investigation of the T_2 relaxation times variations* – by conducting serial examinations at predetermined intervals and follow-ups after radiotherapy, it is possible to gain a deeper understanding of the immediate and delayed changes in the prostate gland.
- *Contribution to personalized medicine* – the study identified varied patterns among patients, demonstrated by the delayed decrease in T2 relaxation times in specific cases. Therefore, the adoption of this quantitative approach could greatly contribute to the development of personalized cancer monitoring systems.

2. Material and methods

The purpose of this paper is to explore the T_2 relaxation times in patients undergoing radiotherapy. The study provides an in-depth analysis of the changes in these times as well as their potential correlation with therapeutic outcomes. For a simplified overview of the study, please refer to Fig. 1, which presents a diagrammatic representation of the study setup.

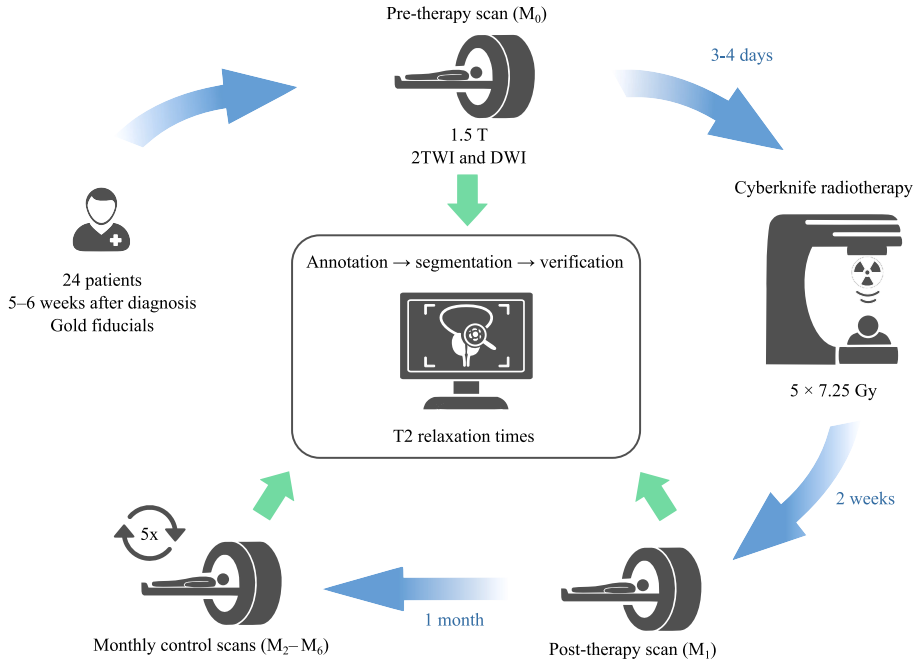

Fig. 1. A simplified study workflow - A visual summary of the research design and methodology employed in the study, detailing patient selection, therapy application, MR examinations and MR data analysis.

2.1. Patients characteristics

A total of 24 patients (mean (standard deviation) age: 72.96 (6.29) years, age range: 61 – 85 years) who underwent radiotherapy using Cyberknife for low-risk and intermediate-risk prostate cancer were selected (Gleason score (GS) 3 + 3 and 3 + 4, staging T1, N0 or T2aN0). All participants included in the study did not undergo any other treatment for prostate cancer and were patients of the Oncology Clinic of the University Hospital in 2020-2022. All patients underwent implantation of gold fiducials for navigation for the Cyberknife (fiducials are not a contraindication for MR imaging and radiotherapy according to studies [23,24]). Patients with previous chemotherapy, radiotherapy or hormone replacement therapy were excluded. Informed consent form was obtained from all subjects and this study was approved by the Ethics Committee of University Hospital Ostrava, 17. listopadu 1790, 70852 Ostrava-Poruba, Czech Republic (Reference number: 967/2019).

2.2. Therapy

Treatment was started within 5-6 weeks from diagnosis. The gold fiducials were introduced for the navigation of robotic radiotherapy 3 or 4 days prior the actual irradiation. Radiation treatment was then carried out in five sessions with a total dose of 36.25 Gy, individual sessions with a dose of 7.25 Gy, 3 sessions per week.

2.3. Magnetic resonance examinations

MR image acquisition was performed using a 1.5T MRI (Magnetom Avanto, Siemens, Erlangen, Germany). Patients were in the supine position and were examined using a 4-channel body coil placed over the pelvic region. The MRI protocol consisted of axial T_2 weighted, axial diffusion weighted imaging (DWI) and multiecho T_2 weighted images for quantitative T_2 mapping. The imaging parameters are listed in Table 1.

The initial MRI measurement (M_0) was planned prior to commencing the radiation therapy. The procedure was performed after the placement of gold fiducial markers within the prostate for the purpose of aligning the image and providing a guidance throughout the treatment process, ensuring precise targeting, and minimizing potential side effects. The follow-up MRI measurement (M_1) was planned for two weeks after radiation therapy ended. This provided adequate time for the treatment effects to manifest and be accurately evaluated.

After the post-therapy MRI scan, five additional check-ups were arranged (M_2 - M_6), each occurring at monthly intervals to closely monitor any changes or progress. These regular, month-long intervals provided a comprehensive and systematic overview of the patient's condition, allowing healthcare professionals to track the treatment's efficacy and adjust their approach as needed. This consistent monitoring was essential to ensuring the most effective possible outcome for the patient. It provided valuable insights into the effectiveness of radiation therapy.

Table 1
The parameters of the MR sequences used in this study.

Sequence Type	FoV (mm)	TE (ms)	TR (ms)	Matrix size	Voxel size (mm)	Flip Angle (°)
Axial T2w TSE	200	89	3440	256x205	1.0x0.8x3.0	150
DWI EPI	221	92	400	160x112	2.3x1.6x3.0	90
T2maps SE	230	22, 44, 66, ..., 352	3000	256x197	1.2x0.9x5.0	180

Note: TSE – turbo spin echo, T2W – T2-weighted, DWI – diffusion weighted imaging, EPI – echo-planar imaging, SE – spin echo, FoV – field of view, TE – echo time (in T2 maps starting echo 22 with step of 22 up to 352 ms), TR – repetition time.

2.4. MR data analysis

A comprehensive analysis of the MR images of all 24 patients was conducted under the supervision of a radiological expert, P.H., who has more than 20 years of experience in the field. As a first step, the MRI images were loaded into ITK-SNAP, a widely used medical image analysis software program [25], wherein the lesions indicative of prostate cancer (PCa) were meticulously identified and demarcated manually on an initial measurement (M_0) prior to radiation therapy. In order to ensure continuity and consistency of the analysis, the manually created annotations from the initial measurement were replicated on subsequent image sets. These annotations were then manually modified by MR image analysis expert (D.V., 5+ years of experience) to account for any discernible deformations or displacements in the prostate gland or lesions. Each set of images belonging to each patient was meticulously reviewed and adapted.

Additionally, a trained medical student V.S. manually segmented the entire prostate gland. In accordance with the procedure used for the segmentation of PCa lesions, the segmentation process was rigorously verified by the radiologist, P.H. By implementing this meticulous process, we ensured that the segmentation and annotation process would be accurate and reliable, thereby providing a robust foundation for analysis of the data. The regions of interest (ROIs) identified in each patient were subjected to an in-depth quantitative assessment. The T_2 relaxation times were determined by analyzing T_2-weighted multiecho scans. To provide a comprehensive representation of tissue properties, a total of sixteen echos were incorporated into this study. It is worth noting that the first echo was systematically omitted from the analysis. The removal of the first echo is a common technique in quantitative MRI since it often contains significant system imperfections, allowing for a more robust and reliable fitting of the T_2 relaxation times [26]. The fitting process of T_2 relaxation curve was carried out using an in-house MATLAB (MathWorks, Natick, MA) code, on a voxel-by-voxel basis. The fitted T_2 relaxation times were then used as the basis for further analysis. By using this approach, we were able to extract detailed and clinically relevant information from the T_2-weighted multi-echo scans allowing better understanding of the radiotherapy impact [27].

2.5. Statistical analysis

For each of the 24 subjects included in the study, T_2 median values were calculated for the entire prostate. Nevertheless, three subjects were excluded from the statistical analysis as a result of MR artifacts or missed appointments, resulting in a final total of 21 subjects being included. The data were first assessed for normality using the Shapiro-Wilk tests. This test showed that the data were not normally distributed, and hence, a log transformation was applied to correct this. After applying the log transformation [28], data with p-values less than 0.05 were considered to indicate a statistically significant difference. Then, we performed a Repeated Measures Analysis of Variance (RM-ANOVA) to examine the significance of differences in T_2 median values between the seven measurements. This analysis controls subject-level variability and is appropriate for our study design where the same subjects were measured repeatedly. The RM-ANOVA was followed by post-hoc pairwise t-tests to understand where these differences lay. Considering the large number of pairwise comparisons, the Bonferroni correction was applied. A p-value (after Bonferroni correction) less than 0.05 was considered statistically significant.

3. Results

Our findings demonstrated a significant association between T_2 relaxation times of entire prostate and quantifiable changes. Specifically, The RM-ANOVA demonstrated a statistically significant difference in the T_2 median values of prostate across the seven measurements ($F(6, 120) = 0.611$, $p << 0.001$, $\eta^2 = 0.305$). This suggests that there is a significant effect of measurement time point on T_2 median values. The MRI measurements are denoted as $M_0 - M_6$, where M_0 is the initial measurement prior the radiotherapy and M_1 - M_6 are the follow-up measurements (M_1 - two weeks after radiotherapy, M_2 - M_6 monthly interval check-ups).

The post-hoc tests with Bonferroni correction revealed that T_2 median values of prostate were significantly different at baseline (M_0) as well as at all other measurement points (M_1 - M_6). Specifically, a statistically significant difference was found between M_0 and M_1 ($T(20) = 4.97$, $p = 0.0016$). This difference continued to increase over time with T_2 median values from M_0 significantly differing from M_2 ($T(20) = 10.23$, $p < 0.001$), M_3 ($T(20) = 12.56$, $p < 0.001$), M_4 ($T(20) = 11.61$, $p < 0.001$), M_5 ($T(20) = 10.49$, $p < 0.001$), and M_6 ($T(20) = 12.33$, $p < 0.001$). Interestingly, a significant difference in T_2 median values of prostate was also observed between M_1 and the following time points: M_3 ($T(20) = 3.94$, $p = 0.017$), M_4 ($T(20) = 3.68$, $p = 0.031$), M_5 ($T(20) = 3.53$, $p = 0.044$), and M_6 ($T(20) = 3.42$, $p = 0.057$). However, there was no significant difference observed between M_1

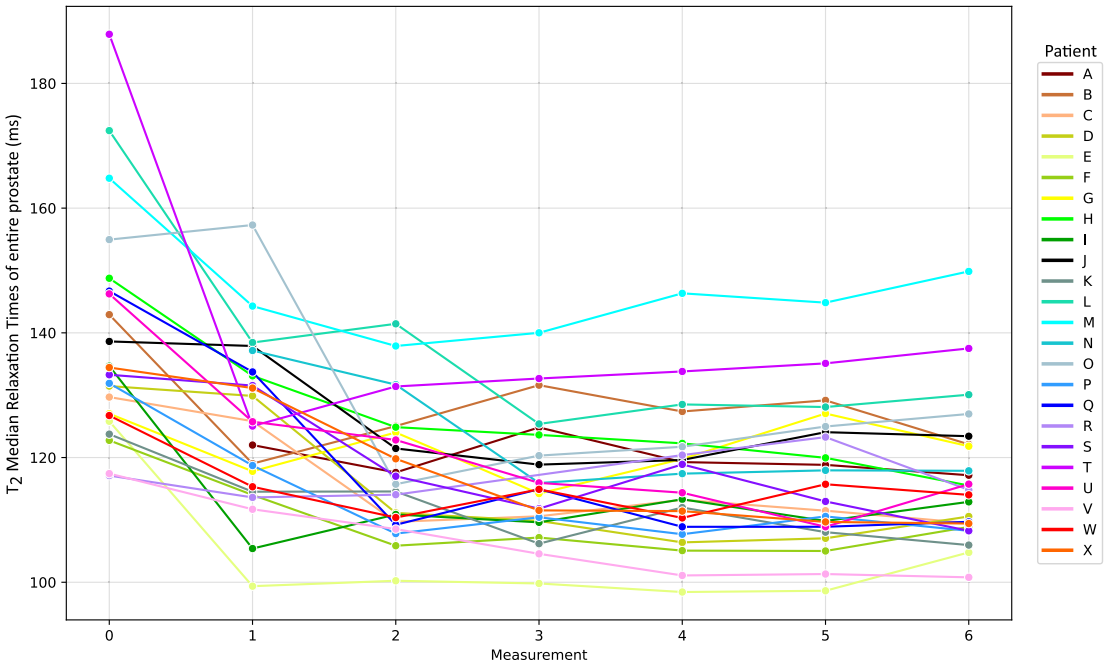

Fig. 2. Longitudinal changes in T_2 median relaxation times of entire prostate gland across all patients (A – X) and measurements. Measurement 0 – initial scan before radiotherapy (M_0). Measurement 1 – first check up two weeks after radiation therapy ended (M_1) and Measurement 2 – 6 monthly intervals check up (M_2 – M_6).

and M_2 after Bonferroni correction (T (20) = 3.01, p = 0.146). These results suggest a consistent decrease in T_2 median values from baseline (M_0), with the exception of M_1 to M_2 where the changes were not statistically significant. For additional details, refer to Table S1 in the Supplementary Materials.

Fig. 2 illustrates the variation in T_2 median relaxation times of prostate across different measurements. For most patients (denoted using the letters A – X), the most substantial change occurs between baseline (M_0) and the first follow-up measurement (M_1). However, it should be noted that some patients (e.g. patients C, G, and M) exhibit a delayed response, with the greatest change occurring between M_0 and the second follow-up (M_2). This emphasizes the inter-individual variability in response to radiotherapy and highlights the importance of longitudinal monitoring to adequately capture this heterogeneity.

Furthermore, we visualized the changes in T_2 median relaxation time using a heatmap, as shown in Fig. 3, where each row corresponds to a specific patient (A – X), and each column represents an individual measurement time point (M_0 – M_6). Each cell in the heatmap is colored according to its median T_2, with darker colors indicating higher values. It provides a comprehensive, color-coded overview of the shifts in T_2 values across the patient cohort and measurement points, allowing for an at-a-glance comparison of quantifiable changes.

Case studies of two patients, namely patient M and T (Fig. 4) offer more detailed insights into T_2 relaxation times changes, reflecting different tissue composition after radiotherapy. Patient M (74 years old, GS 3+3, T2aN0) exhibited a delayed decrease in T_2 relaxation times, notable in the later measurement time points of the T_2 maps. Despite this initial delay, both diffusion restriction, as seen in the DWI, and a decrease in PSA levels indicate an effective, although prolonged, therapeutic response. Conversely, patient T (71 years old, GS 3+3, T1N0), who had higher baseline T_2 median values, demonstrated a 33.44% change in T_2 median values between the baseline (M_0) and first follow-up (M_1). That was visually apparent in the T_2 maps and marked one of the most significant variation in our study cohort. This implies that T_2 relaxometry techniques could be a valuable tool in the monitoring of radiotherapy for low-risk and intermediate risk prostate cancer patients.

4. Discussion

The results of both the statistical analysis and imaging visualizations demonstrate distinct patterns of quantifiable changes after radiotherapy by CyberKnife among patients. As evidenced by the line graph in Fig. 2, the most substantial changes in T_2 median relaxation times typically occur between the M_0 and M_1, with the exceptions in some patients where the most significant changes occurred between M_0 and M_2. This is further highlighted using the heatmap of T_2 median values (Fig. 3) which provides at-a-glance comparison of quantifiable changes suitable for clinical practice usage.

T_2 relaxometry is a method providing insights into water content of the examined tissue. However, one must keep in mind that a prostate tumor is not the only pathology that can be present in the prostate examined [29]. It can be expected that the subjects involved in this study also suffered from prostatitis: acute or chronic. Acute prostatitis is associated with a higher proportion of water whereas chronic one is linked with higher proportion of fibrosis leading to reduction of T_2 relaxation times [30]. Another factor playing an important role is the proportion of stromal and glandular hyperplasia, which has more water than hypertrophic

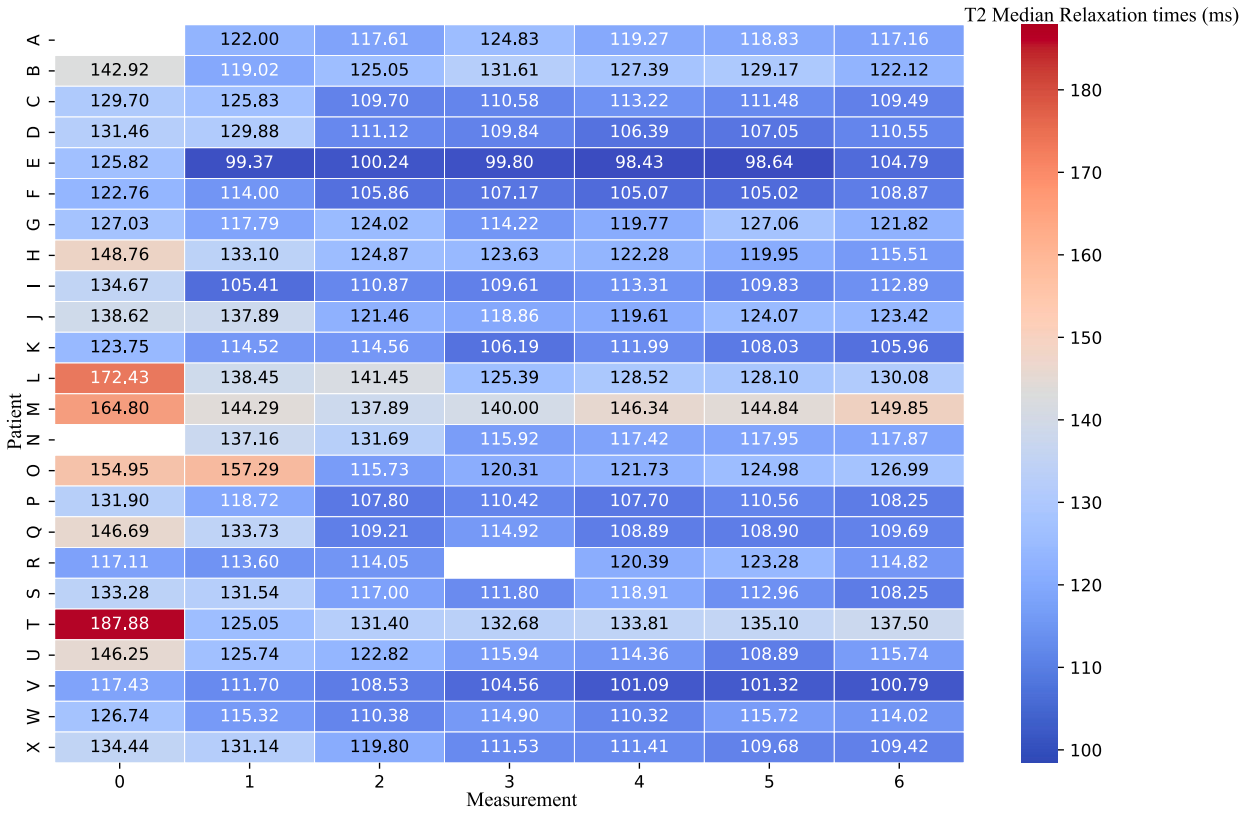

Fig. 3. Heatmap of T_2 Median Relaxation Times. Each row represents a patient, and each column represents a distinct measurement time point. Darker colors indicate higher T_2 median values, highlighting the pattern of change over time. Note that the absence of data in some cells is a result of either missed appointments or the occurrence of image artifacts.

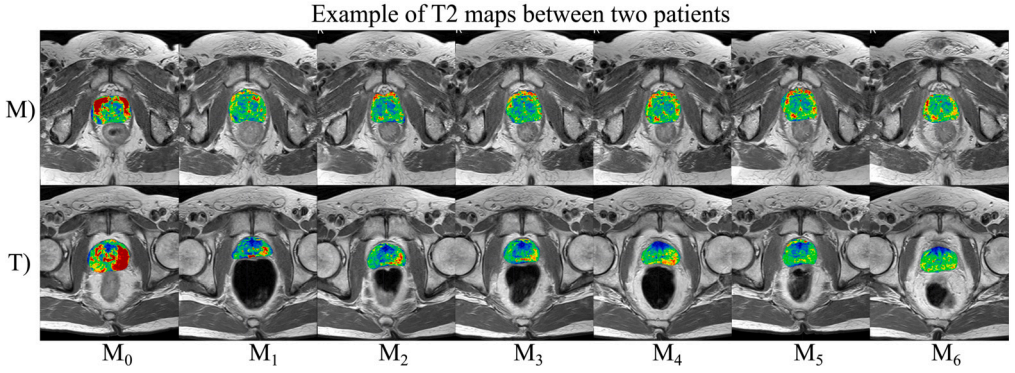

Fig. 4. Comparative T_2 maps of two patients with contrasting quantifiable changes in respective T_2 relaxation times. Each row represents a distinct measurement time point for each patient, with corresponding T_2 maps overlayed. Patient M – 74 years old, Gleason score 3+3, T2a and N0. Shows a delayed decrease in T_2 relaxation times, confirmed with weak RT response, visible in later measurement time points. B) Patient T – 71 years old, Gleason score 3+3, T1 and N0 starting with higher baseline T_2 median values, exhibits a significant change in T_2 median values between baseline (M_0) and the first follow-up (M_1). The T_2 maps visually reflect this marked difference, underscoring the changes in the prostate gland.

stroma [31]. These proportions are variable and cannot be generalized. Therefore, it can be expected that the output for each individual (its range and baseline) will differ as shown in our results.

Another aspect that could affect the results of the start scan was the fact that it was always measured after the implantation of gold fiducials into the prostate, used for navigation of subsequent radiotherapy using the CyberKnife. This application may have been a cause of acute prostatitis in the given patient. In addition, prostatitis is also activated after radiotherapy itself, when some patients develop so-called post-radiation prostatitis, leading to PSA elevations and decreases in the period up to several weeks after radiotherapy.

The prostatitis and its share in the stromal and acinar part greatly changes the resulting relaxation times. For such a limited cohort, it is not possible to correlate individual times, but it is possible to compare their trend, as showed by Foltz et al. [32]. In Foltz's study, the measurements were carried bi-weekly throughout eight weeks of radiotherapy and the results proved that T_2 can serve as a useful biomarker to detect early response to radiotherapy even in patients with low and intermediate risk localized prostate cancer.

A delayed decrease in relaxation times is evident in one patient (M). In this case, a long-term restriction in diffusion was demonstrated in this patient when examined using the DWI, which indicates that the effect of the therapy was prolonged. However, there was a decrease in PSA, which correlates with biochemical markers of therapy effectiveness according to oncological procedures, so this case was not evaluated as a therapy failure.

Finally, the study presented herein offered some valuable insights but also faced several limitations, for example, the absence of a control group or reference from histopathological evaluation. The main reason for not obtaining a detailed histopathological evaluation and a deeper specification of the tumor tissue distribution was not performed, because the radical surgical procedure was found unnecessary in these patients due to low grade staging. Therefore, the entire prostate volume was not processed. Because of low staging, only a needle biopsy was performed and radiotherapy was initiated.

As a result of the collection of biopsy samples, it is not possible to describe in detail the distribution and specification of tumor cells within the tumor mass, but only to provide a rough estimate of the patient's prognosis based on a risk stratification. The reason for this is that samples are taken from different parts of the prostate, which (despite the large number of samples taken) does not cover the entire organ and does not represent the tumor tissue, as it would if the entire prostate was removed [33]. Moreover, in the cases when a less risky part of the tumor was removed during the prostate biopsy, the determined Gleason score may not correspond to the real risks and prescribed treatment (e.g. cases of misdiagnosed multifocal carcinoma [34]).

Furthermore, instead of selecting the ROI (the tumor) whole prostate was analyzed, which may lead to bias due to other mechanisms and pathologies taking place in the affected organ. However, since the focus of the study was on low-grade tumors, the determination of the ROI is complicated and hardly reproducible for repeated measurements. Additionally, the use of an endorectal coil could significantly enhance the image quality and allow magnetic resonance spectroscopy, however, because of the many repeated measurements, its use has been prohibited.

5. Conclusion

In this study, we used 16 echo times to determine the T_2. This type of calculation is considered very precise. Moreover, the cohort selected consisted of 24 elderly patients with low grade carcinoma, which can be considered as a unique cohort. The patients were scanned 7 times, once before radiotherapy, two weeks after radiotherapy, and then monthly, which provides more reasonable window to monitor quantifiable changes subsequently to the radiotherapy. The main contributions can be summarized as follows:

1. *Quantification of scarring* – description of the scarring process in the tumor in well-responsive tumors.
2. *Analysis of the variations in post-radiotherapy T_2 relaxation times* – the study proved that MRI examinations after radiotherapy can provide insights to the immediate and delayed changes in the prostate gland. It is especially important during the period of post-radiation prostatitis, when extreme PSA elevation does not mean therapy failure.
3. *Investigation of the variations among patients* – the study identified varied patterns among patients, demonstrated, for example, by the delayed decrease in T2 relaxation times in specific cases. Moreover, T_2 relaxometry proved to be promising tool to monitor the quantitative changes to radiotherapy even in unconfirmed, but still at-risk patients.

The changes in T_2 values during the course of radiotherapy can help in uncovering alterations in cancer and prostate tissue more sensitively than other parameters, if monitored and visualized appropriately. The adoption of this quantitative approach could greatly contribute to the development of personalized cancer monitoring systems or machine learning-based tools for precision medicine.

Ethics approval

All procedures performed in studies involving human participants were in accordance with the ethical standards of the institutional and/or national research ethics committee of University Hospital Ostrava (Reference number: 967/2019) and with the Helsinki declaration and its later amendments.

Informed consent

Informed consent form was obtained from all individual participants included in the study.

CRediT authorship contribution statement

Pavla Hanzlikova: Conceptualization, Data curation, Formal analysis, Investigation, Validation, Writing – original draft, Writing – review & editing. **Dominik Vilimek:** Conceptualization, Formal analysis, Investigation, Methodology, Software, Validation, Visualization, Writing – original draft, Writing – review & editing. **Radana Vilimkova Kahankova:** Formal analysis, Investigation, Validation, Writing – original draft, Writing – review & editing. **Martina Ladrova:** Formal analysis, Validation, Visualization, Writing

– original draft, Writing – review & editing. **Valeria Skopelidou:** Formal analysis, Investigation, Writing – review & editing. **Zuzana Ruzickova:** Data curation, Writing – review & editing. **Radek Martinek:** Funding acquisition, Resources, Validation, Writing – review & editing. **Jakub Cvek:** Data curation, Investigation, Supervision, Writing – review & editing.

Declaration of competing interest

The authors declare that they have no known competing financial interests or personal relationships that could have appeared to influence the work reported in this paper.

Data availability

Data will be made available on request.

Acknowledgement

This work was supported by Ministry of Health, Czech Republic - conceptual development of research organization (FNOs/2020) and by the Ministry of Education of Czech Republic under Project SP2023/042.

Appendix A. Supplementary material

Supplementary material related to this article can be found online at https://doi.org/10.1016/j.heliyon.2024.e24557.

References

[1] A.K. Miyahira, A. Sharp, L. Ellis, J. Jones, S. Kaochar, H.B. Larman, D.A. Quigley, H. Ye, J.W. Simons, K.J. Pienta, H.R. Soule, Prostate cancer research: the next generation; report from the 2019 Coffey-Holden prostate cancer academy meeting, Prostate 80 (2) (2020) 113–132, https://doi.org/10.1002/pros.23934.
[2] C. Ritch, M. Cookson, Recent trends in the management of advanced prostate cancer, F1000Res. 7 (2018) 1513, https://doi.org/10.12688/f1000research.15382.1.
[3] Z. Khan, N. Yahya, K. Alsaih, M.I. Al-Hiyali, F. Meriaudeau, Recent automatic segmentation algorithms of MRI prostate regions: a review, IEEE Access 9 (2021) 97878–97905, https://doi.org/10.1109/ACCESS.2021.3090825.
[4] G. Litjens, O. Debats, J. Barentsz, N. Karssemeijer, H. Huisman, Computer-aided detection of prostate cancer in MRI, IEEE Trans. Med. Imaging 33 (5) (2014) 1083–1092, https://doi.org/10.1109/TMI.2014.2303821.
[5] L. Klotz, J. Chin, P.C. Black, A. Finelli, M. Anidjar, F. Bladou, A. Mercado, M. Levental, S. Ghai, S.D. Chang, L. Milot, C. Patel, Z. Kassam, C. Moore, V. Kasivisvanathan, A. Loblaw, M. Kebabdjian, C.C. Earle, G.R. Pond, M.A. Haider, Comparison of multiparametric magnetic resonance imaging–targeted biopsy with systematic transrectal ultrasonography biopsy for biopsy-naive men at risk for prostate cancer: a phase 3 randomized clinical trial, JAMA Oncol. 7 (4) (2021) 534, https://doi.org/10.1001/jamaoncol.2020.7589.
[6] V. Kasivisvanathan, A.S. Rannikko, M. Borghi, V. Panebianco, L.A. Mynderse, M.H. Vaarala, A. Briganti, L. Budäus, G. Hellawell, R.G. Hindley, M.J. Roobol, S. Eggener, M. Ghei, A. Villers, F. Bladou, G.M. Villeirs, J. Virdi, S. Boxler, G. Robert, P.B. Singh, W. Venderink, B.A. Hadaschik, A. Ruffion, J.C. Hu, D. Margolis, S. Crouzet, L. Klotz, S.S. Taneja, P. Pinto, I. Gill, C. Allen, F. Giganti, A. Freeman, S. Morris, S. Punwani, N.R. Williams, C. Brew-Graves, J. Deeks, Y. Takwoingi, M. Emberton, C.M. Moore, MRI-targeted or standard biopsy for prostate-cancer diagnosis, N. Engl. J. Med. 378 (19) (2018) 1767–1777, https://doi.org/10.1056/NEJMoa1801993.
[7] V. Duque-Santana, A. Diaz-Gavela, M. Recio, L.L. Guerrero, M. Peña, S. Sanchez, F. López-Campos, I.J. Thuissard, C. Andreu, D. Sanz-Rosa, V. Achard, A. Gómez-Iturriaga, Y. Molina, E. Del Cerro Peñalver, F. Couñago, Jorge clinical study: 10-year outcomes of risk-adapted radiotherapy defined by multiparametric MRI for prostate cancer, World J. Urol. (Nov. 2023), https://doi.org/10.1007/s00345-023-04682-8.
[8] G. Lemaître, R. Martí, J. Freixenet, J.C. Vilanova, P.M. Walker, F. Meriaudeau, Computer-aided detection and diagnosis for prostate cancer based on mono and multi-parametric MRI: a review, Comput. Biol. Med. 60 (2015) 8–31, https://doi.org/10.1016/j.compbiomed.2015.02.009.
[9] B. Turkbey, A.B. Rosenkrantz, M.A. Haider, A.R. Padhani, G. Villeirs, K.J. Macura, C.M. Tempany, P.L. Choyke, F. Cornud, D.J. Margolis, H.C. Thoeny, S. Verma, J. Barentsz, J.C. Weinreb, Prostate imaging reporting and data system version 2.1: 2019 update of prostate imaging reporting and data system version 2, Eur. Urol. 76 (3) (2019) 340–351, https://doi.org/10.1016/j.eururo.2019.02.033.
[10] N. Schieda, C.S. Lim, F. Zabihollahy, J. Abreu-Gomez, S. Krishna, S. Woo, G. Melkus, E. Ukwatta, B. Turkbey, Quantitative prostate MRI, J. Magn. Reson. Imaging 53 (6) (2021) 1632–1645, https://doi.org/10.1002/jmri.27191.
[11] J. Mai, M. Abubrig, T. Lehmann, T. Hilbert, E. Weiland, M.O. Grimm, U. Teichgräber, T. Franiel, T2 mapping in prostate cancer, Invest. Radiol. 54 (3) (2019) 146–152, https://doi.org/10.1097/RLI.0000000000000520.
[12] A. Panda, V. Gulani, Quantitative imaging of prostate: scope and future directions, in: A. Panda, V. Gulani, L. Ponsky (Eds.), Reading MRI of the Prostate, Springer International Publishing, Cham, 2020, pp. 97–108.
[13] E. Subashi, E. LoCastro, A. Apte, M. Zelefsky, N. Tyagi, Quantitative relaxometry for target localization and response assessment in ultra-hypofractionated MR-guided radiotherapy to the prostate and DIL, Int. J. Radiat. Oncol. Biol. Phys. 114 (3) (2022) S33, https://doi.org/10.1016/j.ijrobp.2022.07.390.
[14] S.C. Deoni, Quantitative relaxometry of the brain, Top. Magn. Reson. Imaging 21 (2) (2010) 101–113, https://doi.org/10.1097/RMR.0b013e31821e56d8.
[15] G. Lemberskiy, E. Fieremans, J. Veraart, F.-M. Deng, A.B. Rosenkrantz, D.S. Novikov, Characterization of prostate microstructure using water diffusion and NMR relaxation, Front. Phys. 6 (2018) 91, https://doi.org/10.3389/fphy.2018.00091.
[16] A.A.O. Carneiro, G.R. Vilela, D.B.D. Araujo, O. Baffa, MRI relaxometry: methods and applications, Braz. J. Phys. 36 (1a) (Mar. 2006), https://doi.org/10.1590/S0103-97332006000100005.
[17] D. Karkar, P. Chaudhari, Cyberknife treatment for different types of tumor, J. Pharm. Res. 8 (2) (2023) 248–252.
[18] Y. Cheng, Y. Lin, Y. Long, L. Du, R. Chen, T. Hu, Q. Guo, G. Liao, J. Huang, Is the CyberKnife © radiosurgery system effective and safe for patients? An umbrella review of the evidence, Future Oncol. 18 (14) (2022) 1777–1791, https://doi.org/10.2217/fon-2021-0844.
[19] T.R. Cushman, V. Verma, R. Khairnar, J. Levy, C.B. Simone, M.V. Mishra, Stereotactic body radiation therapy for prostate cancer: systematic review and meta-analysis of prospective trials, Oncotarget 10 (54) (2019) 5660–5668, https://doi.org/10.18632/oncotarget.27177.
[20] R. Nakamura, T. Hirata, O. Suzuki, K. Otani, N. Kai, K. Hatano, K. Fujita, M. Uemura, R. Imamura, K. Tanaka, Y. Yoshioka, N. Nonomura, K. Ogawa, Stereotactic body radiotherapy using CyberKnife® for localized low- and intermediate-risk prostate cancer: initial report on a phase I/II trial, Anticancer Res. 40 (4) (2020) 2053–2057, https://doi.org/10.21873/anticanres.14162.

[21] V. Borzillo, E. Scipilliti, D. Pezzulla, M. Serra, G. Ametrano, G. Quarto, S. Perdonà, S. Rossetti, S. Pignata, A. Crispo, P. Di Gennaro, V. D'Alesio, C. Arrichiello, F. Buonanno, S. Mercogliano, A. Russo, A. Tufano, R. Di Franco, P. Muto, Stereotactic body radiotherapy with CyberKnife® system for low- and intermediate-risk prostate cancer: clinical outcomes and toxicities of CyPro trial, Front. Oncol. 13 (2023) 1270498, https://doi.org/10.3389/fonc.2023.1270498.

[22] K. Vuolukka, P. Auvinen, E. Tiainen, J.-E. Palmgren, J. Heikkilä, J. Seppälä, S. Aaltomaa, V. Kataja, Stereotactic body radiotherapy for localized prostate cancer – 5-year efficacy results, Radiat. Oncol. 15 (1) (2020) 173, https://doi.org/10.1186/s13014-020-01608-1.

[23] S. Schneider, R.I. Jølck, E.G.C. Troost, A.L. Hoffmann, Quantification of MRI visibility and artifacts at 3T of liquid fiducial marker in a pancreas tissue-mimicking phantom, Med. Phys. 45 (1) (2018) 37–47, https://doi.org/10.1002/mp.12670.

[24] L. Knybel, J. Cvek, T. Blazek, A. Binarova, T. Parackova, K. Resova, Prostate deformation during hypofractionated radiotherapy: an analysis of implanted fiducial marker displacement, Radiat. Oncol. 16 (1) (2021) 235, https://doi.org/10.1186/s13014-021-01958-4.

[25] P.A. Yushkevich, Y. Gao, G. Gerig, ITK-SNAP: an interactive tool for semi-automatic segmentation of multi-modality biomedical images, in: 2016 38th Annual International Conference of the IEEE Engineering in Medicine and Biology Society (EMBC), IEEE, Orlando, FL, USA, 2016, pp. 3342–3345.

[26] D. Milford, N. Rosbach, M. Bendszus, S. Heiland, Mono-exponential fitting in T2-relaxometry: relevance of offset and first echo, PLoS ONE 10 (12) (2015) e0145255, https://doi.org/10.1371/journal.pone.0145255.

[27] A. Chatterjee, A. Devaraj, M. Mathew, T. Szasz, T. Antic, G.S. Karczmar, A. Oto, Performance of T2 maps in the detection of prostate cancer, Acad. Radiol. 26 (1) (2019) 15–21, https://doi.org/10.1016/j.acra.2018.04.005.

[28] J. Osborne, Notes on the use of data transformations, Pract. Assess. Res. Eval. 8 (6) (2019), https://doi.org/10.7275/4VNG-5608.

[29] A. Stabile, F. Giganti, A.B. Rosenkrantz, S.S. Taneja, G. Villeirs, I.S. Gill, C. Allen, M. Emberton, C.M. Moore, V. Kasivisvanathan, Multiparametric MRI for prostate cancer diagnosis: current status and future directions, Nat. Rev. Urol. 17 (1) (2020) 41–61, https://doi.org/10.1038/s41585-019-0212-4.

[30] A.B. Rosenkrantz, S.S. Taneja, Radiologist, be aware: ten pitfalls that confound the interpretation of multiparametric prostate MRI, Am. J. Roentgenol. 202 (1) (2014) 109–120, https://doi.org/10.2214/AJR.13.10699.

[31] J.C. Weinreb, J.O. Barentsz, P.L. Choyke, F. Cornud, M.A. Haider, K.J. Macura, D. Margolis, M.D. Schnall, F. Shtern, C.M. Tempany, H.C. Thoeny, S. Verma, PI-RADS prostate imaging – reporting and data system: 2015, version 2, Eur. Urol. 69 (1) (2016) 16–40, https://doi.org/10.1016/j.eururo.2015.08.052.

[32] W.D. Foltz, A. Wu, P. Chung, C. Catton, A. Bayley, M. Milosevic, R. Bristow, P. Warde, A. Simeonov, D.A. Jaffray, M.A. Haider, C. Ménard, Changes in apparent diffusion coefficient and T_2 relaxation during radiotherapy for prostate cancer, J. Magn. Reson. Imaging 37 (4) (2013) 909–916, https://doi.org/10.1002/jmri.23885.

[33] E. Short, A.Y. Warren, M. Varma, Gleason grading of prostate cancer: a pragmatic approach, Diagn. Histopathol. 25 (10) (2019) 371–378, https://doi.org/10.1016/j.mpdhp.2019.07.001.

[34] A. Ali, A. Du Feu, P. Oliveira, A. Choudhury, R.G. Bristow, E. Baena, Prostate zones and cancer: lost in transition?, Nat. Rev. Urol. 19 (2) (2022) 101–115, https://doi.org/10.1038/s41585-021-00524-7.